Channels: Where Disciplines Meet

Volume 5
Number 1 *Fall 2020*

Article 1

December 2020

Experimental and Numerical Study of Drag Reduction on Elliptical Cylinders Using Surface Grooves

Michael T. Brocker
Cedarville University, mbrocker@cedarville.edu

David J. McDonell
Cedarville University, davidmcdonell@cedarville.edu

Drake L. Pensworth
Cedarville University, dpensworth@cedarville.edu

Joshua J. Swimm
Cedarville University, jswimm@cedarville.edu

Recommended Citation

Brocker, Michael T.; McDonell, David J.; Pensworth, Drake L.; and Swimm, Joshua J. (2020) "Experimental and Numerical Study of Drag Reduction on Elliptical Cylinders Using Surface Grooves," *Channels: Where Disciplines Meet*: Vol. 5 : No. 1 , Article 1.
DOI: 10.15385/jch.2020.5.1.1
Available at: https://digitalcommons.cedarville.edu/channels/vol5/iss1/1

Experimental and Numerical Study of Drag Reduction on Elliptical Cylinders Using Surface Grooves

Abstract

Drag reduction on an object subject to external flow remains a topic of interest due to a wide range of applications. Previous studies showed that grooves on the surface of a circular cylinder lead to drag reduction, which had thus been applied to save energy in various implementations. In the present study, the effects of longitudinal surface grooves with respect to drag reduction on circular and elliptical cylinders were experimentally explored through resin additive manufacturing and a wind tunnel. Significant drag reduction originated by surface grooves was observed. In conjunction with experimental investigations, numerical analyses were performed with computational fluid dynamics (CFD) to examine the physical causes of the drag reduction. The numerical studies included two- and three-dimensional simulations of flow over circular and elliptical cylinders. The turbulent energy and wake regions of flow were discussed. Key factors in drag reduction were the location of the beginning of turbulence or vortices in the grooves, the boundary layer separation angle, and the size of the turbulent wake region. Through the numerical CFD simulations and experimental results, spanwise surface grooves on elliptical cylinders are verified to reduce drag.

Keywords

CFD (Computational Fluid Dynamics), Drag Reduction, Elliptical Cylinders, Wind Tunnel

Experimental and Numerical Study of Drag Reduction on Elliptical Cylinders Using Surface Grooves

Michael T. Brocker, David J. McDonell, Drake L. Pensworth, Joshua J. Swimm

Engineering and Computer Science

Abstract— *Drag reduction on an object subject to external flow remains a topic of interest due to a wide range of applications. Previous studies showed that grooves on the surface of a circular cylinder lead to drag reduction, which had thus been applied to save energy in various implementations. In the present study, the effects of longitudinal surface grooves with respect to drag reduction on circular and elliptical cylinders were experimentally explored through resin additive manufacturing and a wind tunnel. Significant drag reduction originated by surface grooves was observed. In conjunction with experimental investigations, numerical analyses were performed with computational fluid dynamics (CFD) to examine the physical causes of the drag reduction. The numerical studies included two- and three-dimensional simulations of flow over circular and elliptical cylinders. The turbulent energy and wake regions of flow were discussed. Key factors in drag reduction were the location of the beginning of turbulence or vortices in the grooves, the boundary layer separation angle, and the size of the turbulent wake region. Through the numerical CFD simulations and experimental results, spanwise surface grooves on elliptical cylinders are verified to reduce drag.*

Keywords— *CFD (Computational Fluid Dynamics), Drag Reduction, Elliptical Cylinders, Wind Tunnel*

Introduction

In a world of transportation and constant motion, drag induced by air flowing over a body is an adversary of energy efficiency and aeronautical performance. Reducing the drag on an object moving through a fluid is a goal for which many fluid dynamics researchers strive. The most common method of drag reduction is to alter the profile of an object and make it more streamlined. Bluff bodies transformed into more aerodynamic profiles are highlighted in the transportation industry. However, for some applications, the geometry of the body cannot be modified and an alternative method of drag reduction is required.

Such reduction of drag in bluff bodies is the focus of this paper. The study presented is an experimental and

The authors thank the Cedarville University School of Engineering and Computer Science for their support in funding the research presented in this paper.

The authors are with the Mechanical Engineering Department, Cedarville University, Cedarville, OH 45314 USA, as undergraduate senior students.
M. T. Brocker (email: mbrocker@cedarville.edu)
D. J. McDonell (email: davidmcdonell@cedarville.edu)
D. L. Pensworth (email: dpensworth@cedarville.edu)
J. J. Swimm (email: jswimm@cedarville.edu)

numerical analysis of drag reduction on circular and elliptical cylinders.

In a previous investigation of grooved circular cylinders, Song [1] used two-dimensional computational fluid dynamics (CFD) to analyze the flow patterns around the surface of a cylinder and how groove parameters could predictably affect such patterns. They proposed a mechanism of drag reduction to be changes in the flow separation point. The location of this detachment was determined by three groove parameters: the depth of the grooves, the angle α between the upstream stagnation point and the rearmost groove, and the width of the grooves. Song suggested a quadratic relationship between these groove parameters, highlighting an optimal set of parameters for greatest drag reduction.

Rodriguez [2] and Buresti [3] studied numerically and experimentally, respectively, the effects of surface roughness on drag reduction. Their research focused on how surface roughness in varying flow regimes impacts drag and vortex shedding in the wake region. Other drag reduction research has been conducted branching from naturally formed flow profiles. Analyzing cactus surface roughness, Seong-Ho [4] used U-shaped grooves perpendicular to the flow to reduce drag over bluff bodies. They found that using a few grooves at an angle of approximately 90° from the upstream stagnation point yielded reductions up to 28% compared to smooth circular cylinders. Yunqing [5] researched drag reduction from the textured skin in some aquatic creatures.

The desire to reduce drag is pervasive across the world of fluid mechanics. This paper presents an experimental and numerical analysis of circular and elliptical cylinders at a Reynolds number of $6 * 10^4$ and suggests an explanation regarding the specific mechanisms of drag reduction.

Terminology and Methodology

For clarity and succinctness in referencing groove parameter styles, some main terms adapted from [1] will be used to generally describe a cylinder's cross section. The term "grooved cylinder" describes, in general, a right cylinder with lengthwise grooves which are parallel to the central axis of the cylinder such that a cross section through the central axis is the same at any point on the cylinder. "Smooth Model" describes a cylinder with no grooves around its perimeter. "Model A" is a cylinder with evenly spaced grooves surrounding its cross section's entire perimeter with the groove pattern centered at the upstream stagnation point. "Model B" is also grooved and centered at the upstream stagnation point, but it is only grooved (nominally) on the upstream side of the cylinder with the rearmost groove located at an angle α from the stagnation point. Unless otherwise specified, α is assumed to be 90° for Model B. Fig. 1 shows cross sections of Models A and B.

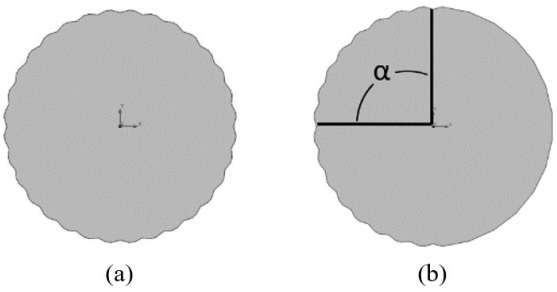

Fig. 1 Cross section of circular (a) Model A and
(b) Model B for α = 90°

Physical Experimentation

A. Experimental Procedure and Approach

The experimental analysis consisted of a calibration assessment of the equipment, fabricating physical models, and testing the manufactured circular and elliptical cylinders.

The force measurement device was designed by M. Bird [6] for reading small forces in a wind tunnel. The measurement apparatus, referred to as the low drag cart, (Fig. 3) used a pulley system to transfer a drag force to a weight resting on a scale outside of the wind tunnel. Suspended by a steel fork, the test specimen was held in front of the testing apparatus to receive uniform flow. The post holding the fork was cased in a symmetric air foil to reduce the drag influence from the mounting elements. The weight on the scale was recorded before the test began and while the wind tunnel ran at the desired speed. The difference of the readings on the scale was the drag force on the mounting elements and the test specimen combined. Then the drag without the specimen was measured and subtracted from the previous value, eliminating the bias error from the vertical post's drag.

To verify that the low drag cart accurately measured the drag force of the mounted specimen, two types of objects were tested. The first was a round, thin disk with a face perpendicular to the flow. Because thin disks are well studied shapes in fluid mechanics [7], this was the primary means of assessing the testing procedure. The first verification test yielded results within 10% of the published values, indicating that the low drag cart was nominally accurate.

The second verification procedure included 150 mm long cylinders with outer profiles correlating with the smooth model, Model A, and Model B. The physical models had the same cross section as those studied in [1], but the diameter was scaled up by 1.5 (from 25.4 mm in [1] to 38.1 mm) in order to achieve the same Reynolds number used in [1] while keeping the required wind speed within a range acceptable for the wind tunnel in use (23.3 m/s instead of 35 m/s in [1]). After verifying through dimensional analysis [7], the groove parameters were scaled proportionally to the cylinder diameter.

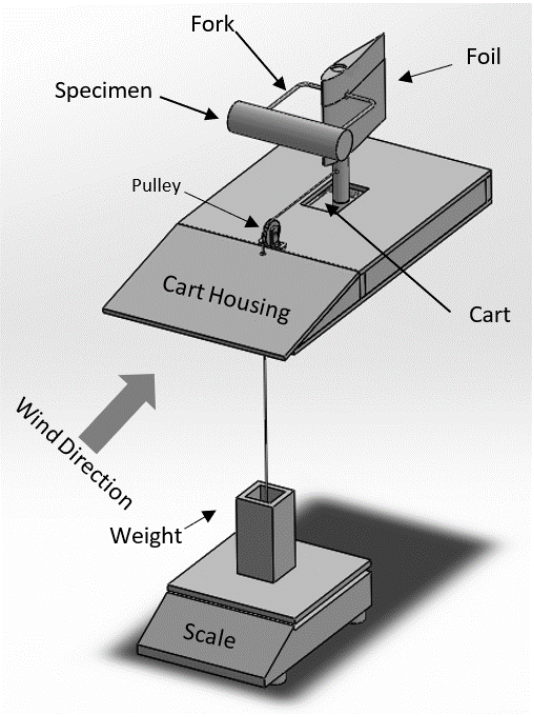

Fig. 3 Low Drag Cart

Throughout the physical testing, the groove parameters were varied to isolate the effects of certain characteristics, but unless otherwise stated, the grooves were 2.8 mm in width, 0.39 mm in depth and spaced evenly with 11.25° between the deepest part of each groove. The cylinders were fabricated using resin 3D printing to obtain detailed groove profiles difficult to manufacture conventionally or with fused deposition modeling (FDM) 3D printing.

These circular cylinders were tested and compared to the research published in [1]. The purpose of this procedure was to determine if the low drag cart was capable of recording the slight changes in drag caused by surface groove drag reduction. However, because the published values [1] used 2D CFD, but the wind tunnel tests included the 3D effect of flow over the ends of the cylinders, the goal for this part of the testing process was to verify that a similar trend could be found. Such a trend was observed, and the data was recorded in Table I.

TABLE I
COMPARING DRAG COEFFICIENTS FROM SONG AND WIND TUNNEL EXPERIMENTATION

Model Type	2D Song [1] C_d	3D Experimental C_d
Smooth	1.21	0.768
Model A	0.83	0.672
Model B	0.785	0.553

Following the verification procedure for the measurement device and wind tunnel, the experimentation transitioned to testing of elliptical cylinders to determine which parameters would optimize drag reduction. In the elliptical models, the varied parameters were the groove depth and number of grooves (N). The aspect ratio for the elliptical model was 0.75 with the minor (vertical) axis length maintained at 38.1 mm and the major (horizontal) axis at 50.8 mm. Instead of using 11.25° as the measurement for groove spacing, the arclength between the groove centers on the circular model (3.7 mm) was used unless otherwise specified. In the circular cylinders, Model B included an angle α to denote how far the grooves went along the surface of the cylinder. For an ellipse, however, the definition of the grooved region for Model B was the total number of grooves. Each model has a groove centered along the stagnation point. Therefore, the number of grooves for Model B is always odd. Fig. 4 shows a representative cross section of the base models used for the elliptical experimentation.

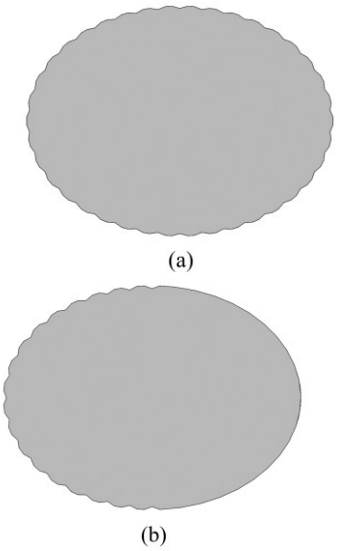

Fig. 4 Cross section of elliptical (a) Model A and
(b) Model B for N=19

The characteristic length for flow over an ellipse is the major axis. To maintain the same Reynolds number of $6 * 10^4$ between the elliptical and circular models, the wind speed over the elliptical models was reduced from 23.3 m/s to 17.3 m/s.

B. Experimental Results and Analysis

The first experimental study on elliptical cylinders examined the depth of the grooves. The groove depth was varied from 1.02 mm to 4.06 mm. The maximum drag reduction occurred at a groove depth of 2.03 mm. This depth yielded a drag reduction of 53% from the smooth elliptical cylinder. This data is recorded in Table II and in Fig 5. For the error, the average standard deviation of the coefficient of drag was 0.0560 for the groove depth study and is also displayed in Fig. 5.

TABLE II
EXPERIMENTAL GROOVE DEPTH STUDY

Groove Depth (mm)	Coefficient of Drag
0	0.4879
0.51	0.4222
1.02	0.2879
2.03	0.2293
3.05	0.2707
4.06	0.4379

The second study varied the number of grooves for Model B while maintaining the groove depth constant at 1.02 mm. The elliptical cylinder with 21 and 23 grooves both showed significant drag reduction compared to the smooth model of 36%. The coefficient of drag, in the groove study, yielded a greater average standard deviation during testing with a value of 0.0586. The data for the groove number study can be seen in Table III and Fig. 6. Both parameters resulted in drag reduction, but the depth of grooves had a greater effect on reducing the coefficient of drag. This trend seen in elliptical cylinders parallels Song's suggestion in [1] that groove depth most significantly impacts the drag reduction and that a quadratic relationship exists between the parameters and drag reduction. The plotted data in Figs. 5-6 suggest that such quadratic relationships exist in elliptical cylinders in addition to the circular models in [1].

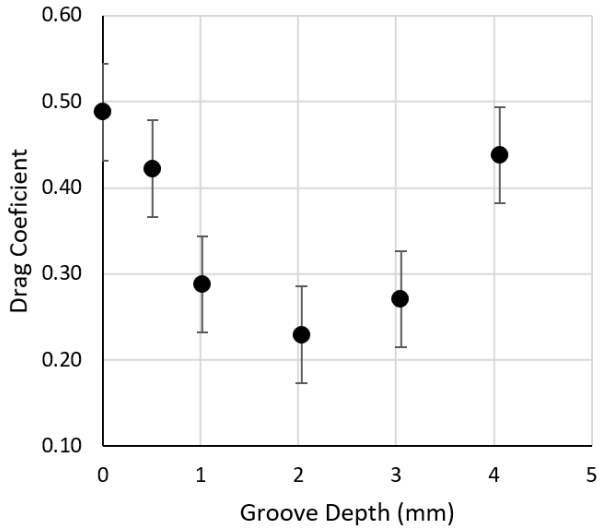

Fig. 5 Groove depth study of elliptical Model A cylinders

TABLE III
EXPERIMENTAL GROOVE NUMBER STUDY

Number of Grooves	Coefficient of Drag
0	0.4879
19	0.3308
21	0.3136
23	0.3179
25	0.3729

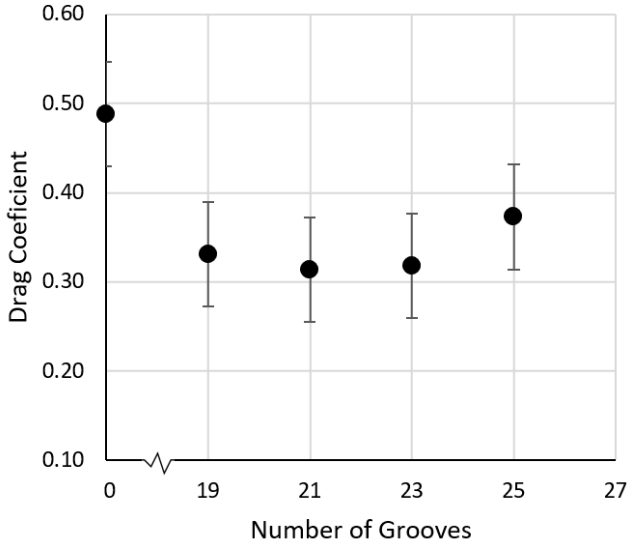

Fig. 6 Groove number study of elliptical Model B cylinders

Numerical Simulation

A. Numerical Procedure and Approach

The numerical research included studies using two and three dimensional CFD in ANSYS FLUENT. Two dimensional simulations were used to provide quick simulations to reveal essential features of the flow fields. Three dimensional simulations were far more expensive in terms of computation time and were used to more accurately simulate the tests in the wind tunnel, as they accounted for the flow over the ends of a non-infinite cylinder.

Both the two- and three-dimensional studies were performed using FLUENT and the meshes were generated in ICEM. To decrease computation time on simulations, calculations were performed at the Ohio Supercomputer Center [8]. The basic setup used consisted of transient turbulent models using a time

step size of 0.0001 s and 2000 time steps for a total flow time of 0.2 s.

The turbulent model used was the Transition SST (Shear Stress Transport) model because of the reliability it holds in regard to external flow over a body [4].

The drag force was calculated using surface integration of the pressure and shear stress on the cylinder surface at each element in the mesh on the boundary. Wang [9] proposes two alternative methods for drag force calculations that were used as the second and third methods in this study. The second method used wake integration to calculate the change in pressure and momentum across the cylinder.

$$D = \int [p_\infty - p_{wake} + \rho u_{wake}(U_\infty - u_{wake})]\, dA \quad (1)$$

The third method is the entropy generation method where

$$D = \frac{T_\infty}{U_\infty} \int_\Omega \dot{s}_{gen}\, d\Omega \quad (2)$$

and where

$$\dot{s}_{gen} = \frac{\mu_{eff}}{T} \left\{ \frac{\partial u_i}{\partial x_j} + \frac{\partial u_j}{\partial x_i} \right\} \frac{\partial u_i}{\partial x_j}. \quad (3)$$

All three methods were used to ensure an accurate measurement of drag could be found and to attempt to reduce the common overestimation of drag from CFD. However, neither the wake integration and entropy generation method gave consistent results for 2D or 3D CFD. Therefore, the surface integration method was selected for force calculations in the numerical analysis.

B. Numerical Study

For the 2D simulations, ANSYS ICEM was used to create the meshes that would be run in ANSYS FLUENT. Most meshes for the 2D study numbered about 104 thousand elements over the computational domain. The mesh was refined around the surface of the cylinders to resolve the flow field in boundary layer. Fig. 7 shows the computational domain around the cylinder.

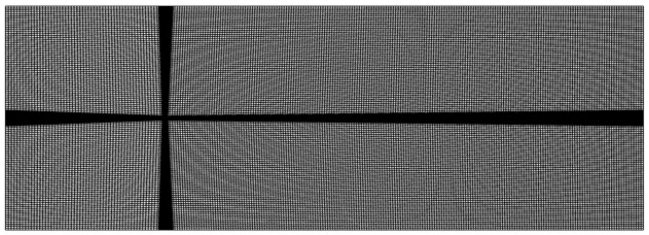

(a)

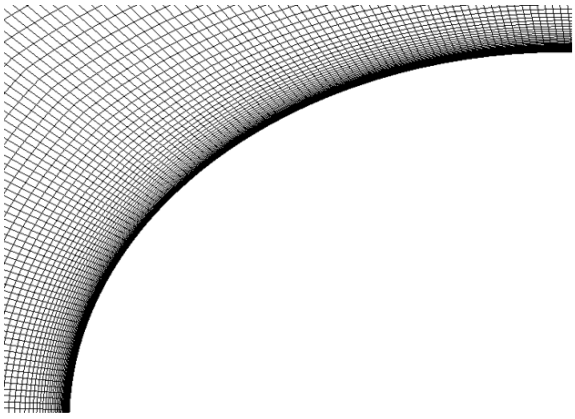

(b)

Fig. 7 Smooth 2D elliptical cylinder mesh (a) entire computational domain (b) surface of cylinder

The two-dimensional CFD study of circular cylinders showed a trend of drag reduction using various groove configurations along the surface. To conduct the study, Song's [1] cases were followed by duplicating their cylinder diameter and groove parameters such as depth, width, and α. Using a Reynolds number of $6 * 10^4$ and a windspeed of 35 m/s, we found similar drag reduction as shown in Table IV. Fig. 8 compares the wake regions behind the cylinder of the smooth model, Model A, and Model B. In Fig. 8, a reduction in the area of the velocity wake region can be observed that correlates with the lower drag coefficients found in Table IV.

TABLE IV
NUMERICAL DRAG COEFFICIENTS FOR CIRCULAR CYLINDERS

Model	Numerical	2D Song [1] C_d
Smooth	1.393	1.21
Model A	0.746	0.83
Model B	0.724	0.785

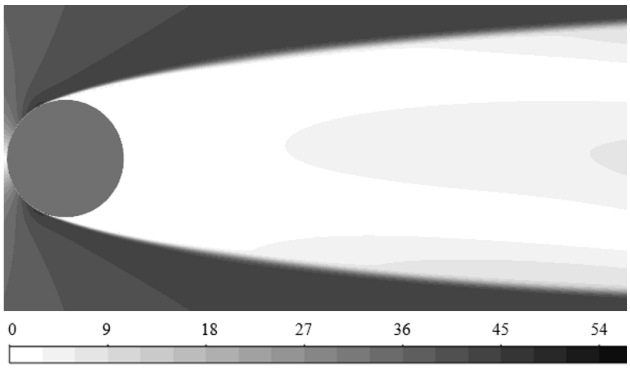

(a)

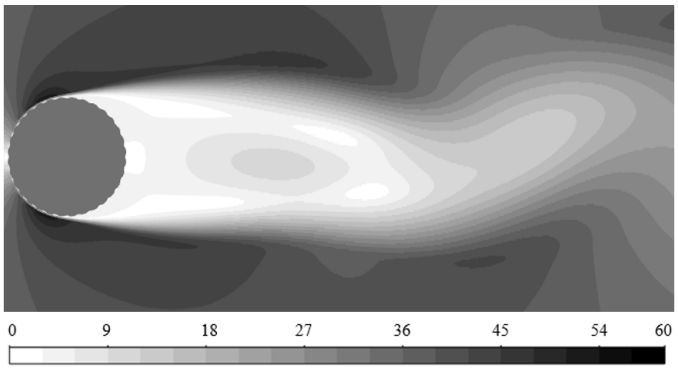

(b)

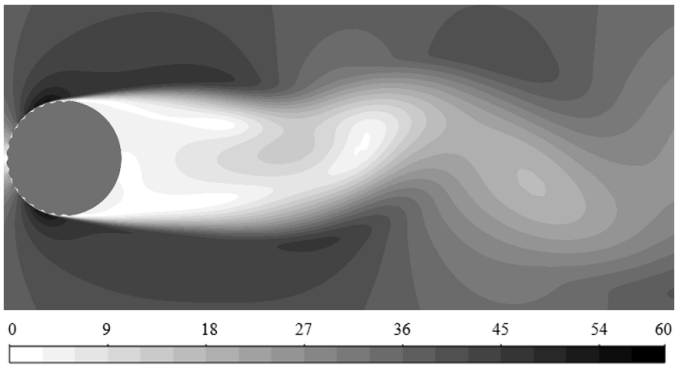

(c)

Fig. 8 Velocity (m/s) wake region behind 2D circular (a) smooth cylinder (b) Model A and (c) Model B

A closer look at the surface of the different models shows that, as the grooves are added to the surface, the wake detaches at a lower angle from the cylinder. This difference can be seen in Fig. 9 as the angle of detachment of the flow decreases from the smooth when compare to the other models. Fig. 9 also shows a more gradual velocity transition in the wake region in Models A and B versus the stark contrast between high and low velocity in the smooth cylinder wake. Table IV supports the hypothesis that reduced wake region and detachment angle of flow correlate to the reduction of drag around a body.

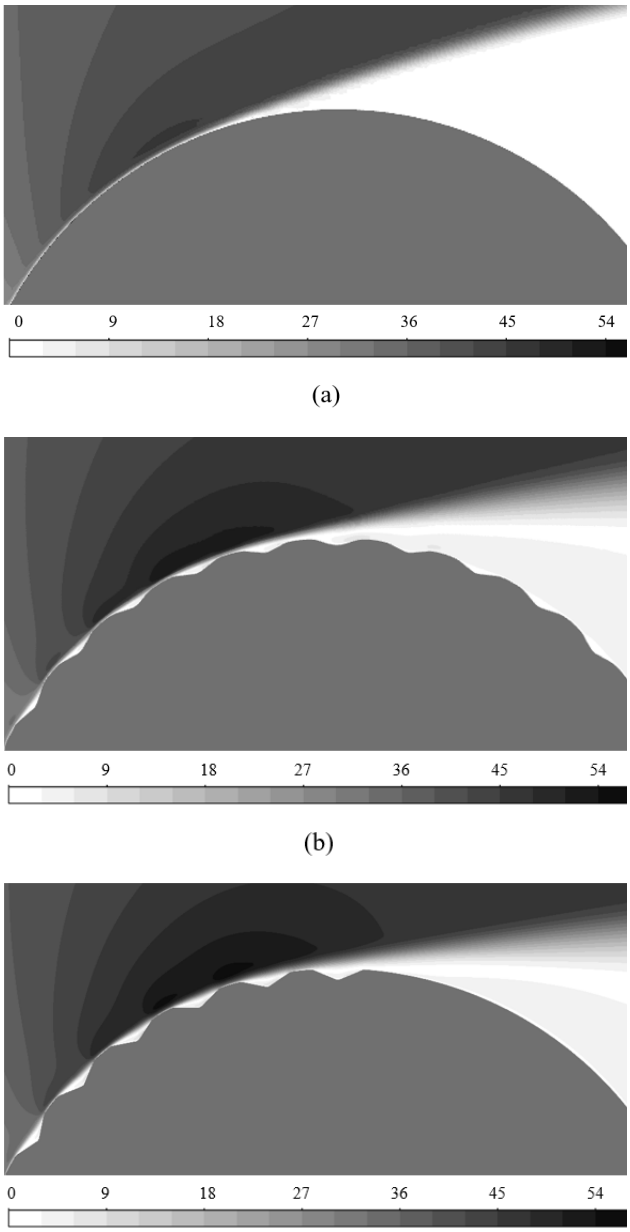

Fig. 9 Velocity (m/s) separation from surface of 2D circular (a) smooth cylinder (b) Model A and (b) Model B

Song [10] suggested that turbulence in the grooves could act as a sort of "bearing" for the air to roll over the cylinder surface. Fig. 10 shows turbulence induced in the grooves, similar to what Song [10] found in his study. In Fig. 10b, Model B is shown to have turbulence developing early on in the grooves and seen in Table IV, Model B showed the greatest drag reduction.

The two-dimensional circular cylinder study showed expected trends as the turbulence found in the grooves corresponded to a lower angle of detachment and thus a smaller wake region behind the cylinder. The driving cause of this drag reduction seems to pertain to the existence of turbulence in the grooves.

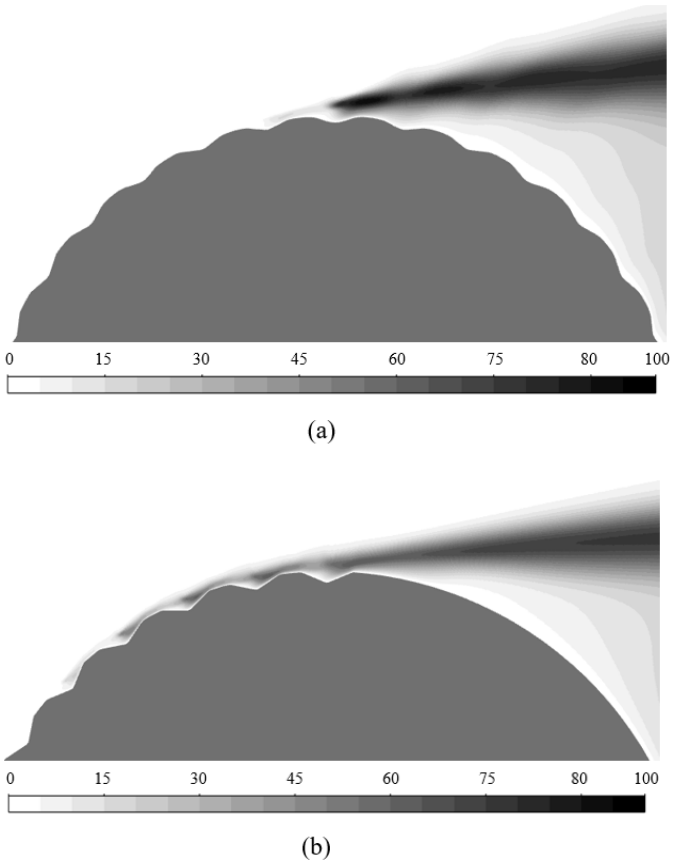

Fig. 10 Turbulent kinetic energy (J/kg) contours for 2D circular (a) Model A and (b) Model B

Two-dimensional CFD was performed on both smooth elliptical cylinder and Model

A to determine if the experimental trend could be reproduced in the numerical study. Although 2D simulations do not address the 3D effect, a trend can be found in the simulations that aligns with the experimental data.

During the analysis, turbulent models for elliptical cylinders were showed to be less stable than for the circular models. To enhance stability and convergence, laminar model was used for elliptical cylinder simulation. To test if vortex formation occurred in elliptical grooves to provide the "bearing" effect discussed in [10], the streamwise velocity along lines normal to the ellipse's surface were plotted. Fig. 11 shows these such lines. The depicted x-values refer to the x-direction distance from the center of the ellipse. The plots use the surface of the cylinder as the origin of the curve to show the velocity as a function of the distance away from the surface. The approach is to look for reversed flow in the grooves which correlates to the presence of vortices.

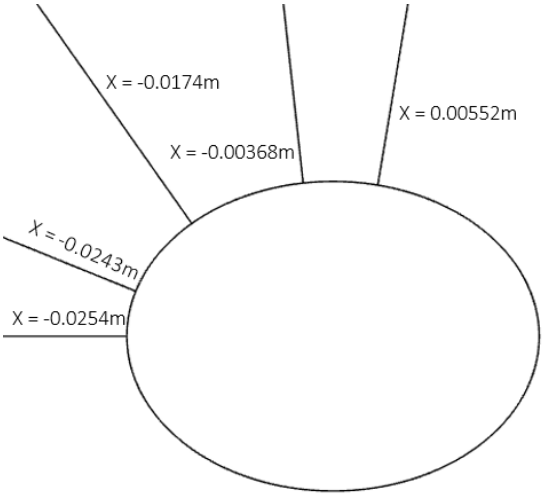

(a)

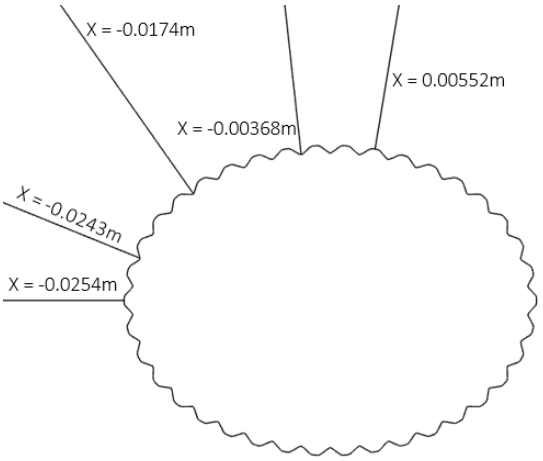

(b)

Fig. 11 Locations of velocity distribution in boundary layer for (a) smooth cylinder (b) Model A

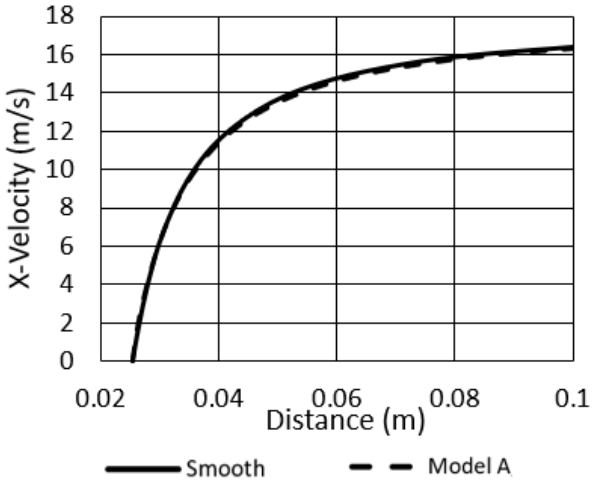

Fig. 12 Velocity distribution in boundary layer for smooth elliptical cylinder and Model A at stagnation point (X = -0.0254m)

Fig. 12 compares the stagnation point boundary layer between both the smooth cylinder and Model A. At the stagnation point it can be seen that the boundary layers for both models correlate closely to each other. Fig. 13 shows that an early reversal of flow began to develop in the grooves of Model A, signaling the

presence of vortices, which then leads to the "bearing" effect around the surface as discussed previously.

Figs 14 and 15 show an increase in the magnitude of reversed flow in the grooves as air moves downstream.

It was not until after the separation point of the smooth cylinder that reversed flow appeared in the boundary layer as seen in Fig. 16. This contrasts the vortices found in the grooves of Model A before the separation point and appears to be directly related to the reduction of drag found in Table V.

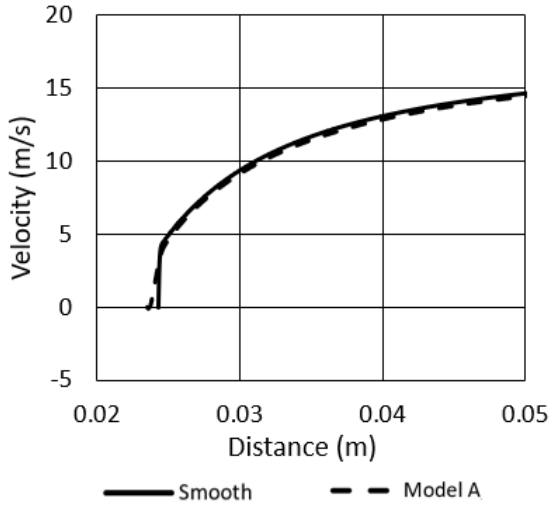

Fig. 13 Velocity distribution in boundary layer (X = -0.0243m)

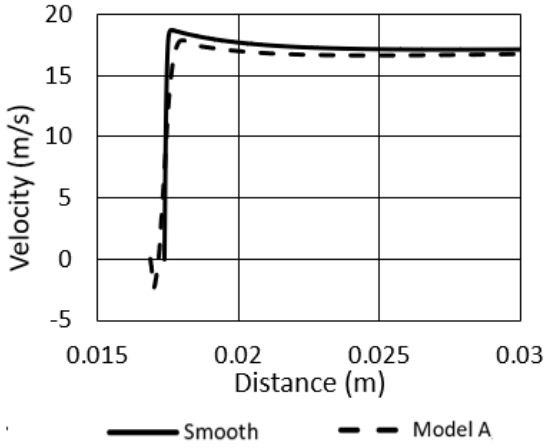

Fig. 14 Velocity distribution in boundary layer (X = -0.01741m)

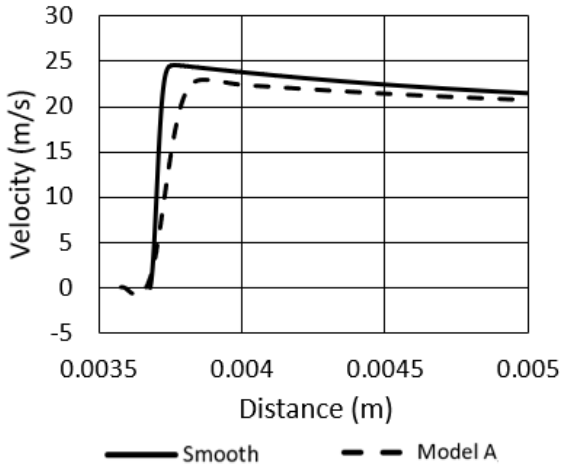

Fig. 15 Velocity distribution in boundary layer (X = -0.00368m)

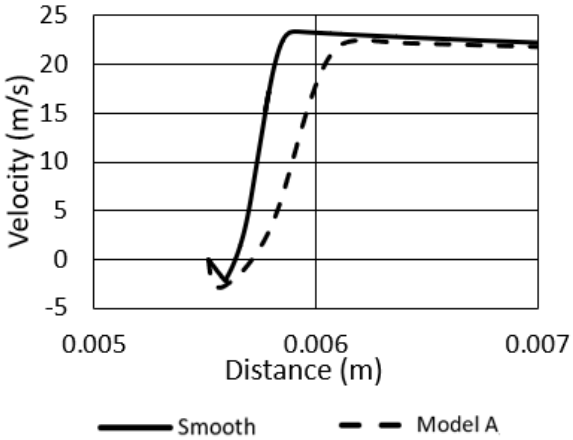

Fig. 16 Velocity distribution in boundary layer after complete separation (X = 0.005515m)

Figs. 17 and 18 show that the detachment angle of the boundary layer decreases from the smooth cylinder to Model A, resulting in a smaller wake region and lower drag (Table V). The laminar model used could not reflect the turbulence in the grooves, but the velocity distribution of the boundary layer in the grooves showed that vortices formed in the grooves produced the "bearing" effect expected that leads to a smaller flow detachment and decreased wake region behind the cylinder. The effect found in these grooves reproduces the same trends that were found in the effect of turbulent vortices that resulted in drag reduction.

TABLE V
DRAG COEFFICIENTS FOR ELLIPTICAL CYLINDERS

Model	Numerical	Experimental
Smooth	0.760	0.488
Model A	0.497	0.288

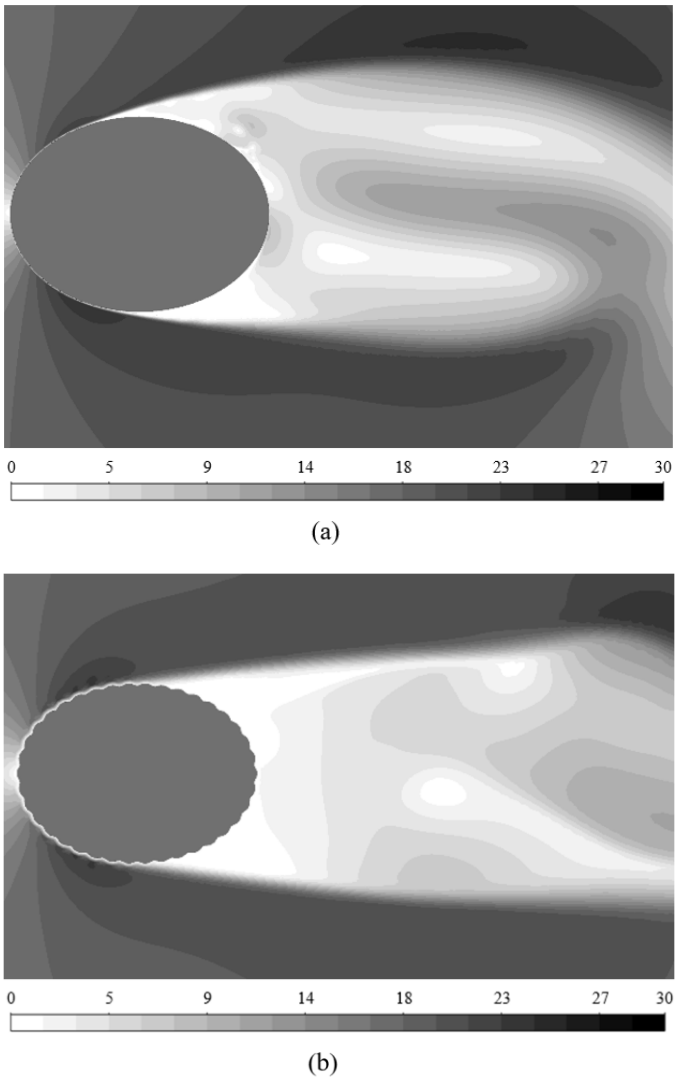

Fig. 17 Velocity (m/s) wake region behind 2D elliptical (a) smooth cylinder (b) Model A

C. Numerical Wake Study

In the three-dimensional studies, the cylinder used in CFD and in the wind tunnel was a 150 mm long circular cylinder with various groove parameters. Song's work [1] used 3D simulations for circular cylinders but the cylinders occupied the entire transverse length of the computational domain which rendered the simulations essentially 2D. In order to show the effects of such

surface grooves in conjunction with flow around the ends of the cylinder, a truly 3D computational domain was used where the ends of a 150 mm long cylinder were away from the computational domain boundaries. Following a mesh convergence study, 9 million elements were found to be sufficient for the 3D simulations. The drag coefficients for the 3D simulations compared to the experimental results are in Table VI.

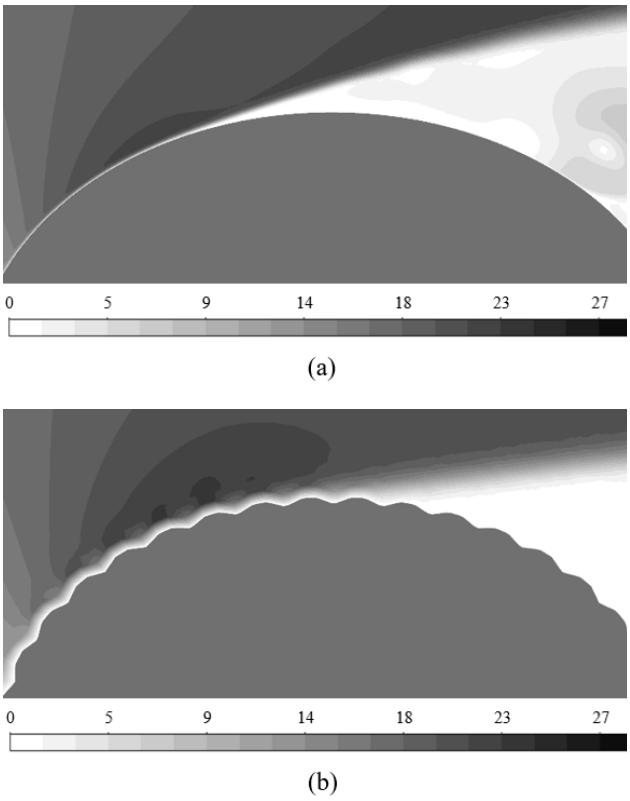

Fig. 18 Velocity (m/s) contour of flow detachment for 2D elliptical (a) smooth cylinder (b) Model A

TABLE VI
3D DRAG COEFFICIENTS FOR CIRCULAR CYLINDERS

	Numerical	Experimental
Smooth	0.699	0.768
Model A	0.642	0.672

The cut plots shown from the 3D simulations in this study were cross sections in the middle of the cylinder axially. Fig. 19 shows cut plots of the turbulent kinetic energy for the smooth cylinder and Model A. Fig. 19 is zoomed in around the separation point of the flow on an amplified scale to highlight flow detachment features. Early groove turbulence was observed in Fig. 19b, showing a gradual transition into turbulence. The model with early induced turbulence also correlated with a decreased angle of detachment of the flow. Fig. 20 shows the velocity profile of the flow pattern and shows (as well as Fig. 19) that the flow detaches more smoothly in the grooved model than the smooth model. The smooth detachment was possibly due to the "roller-bearing" effect of turbulence proposed in [10]. The decreased angle of boundary layer separation in Model A compared to the smooth case resulted, as expected, in a smaller wake region and decreased drag. Fig. 21 shows the velocity wake regions for both cases. Although the two profiles are similar, the wake region for Model A (Fig. 21b) is smaller and the decreased wake size is a key element in the drag reduction observed.

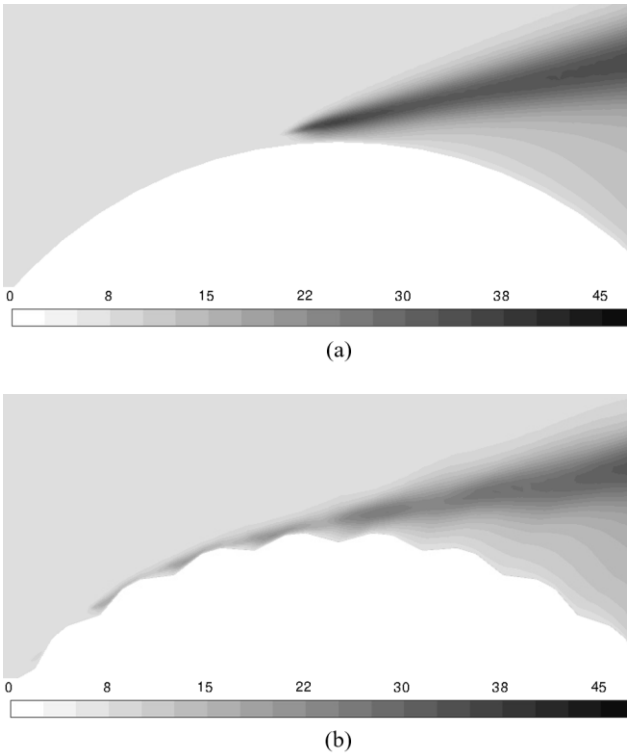

Fig. 19 Turbulent kinetic energy [J/kg] cut plot of detachment region through center of 3D circular cylinder for the (a) smooth case and (b) Model A

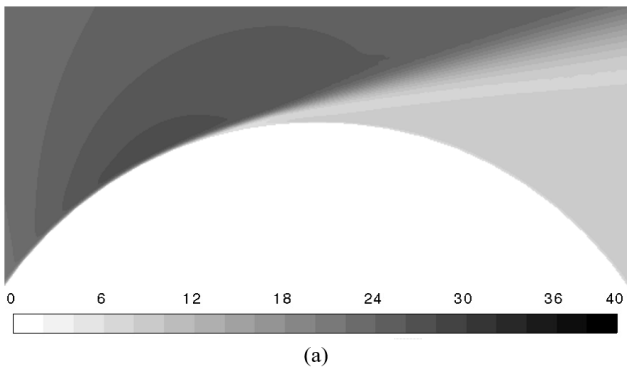

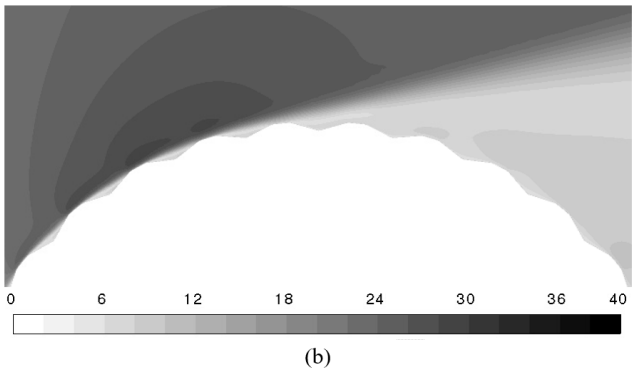

Fig. 20 Velocity magnitude (m/s) cut plot of detachment region through center of 3D circular cylinder for the (a) smooth case and
(b) Model A

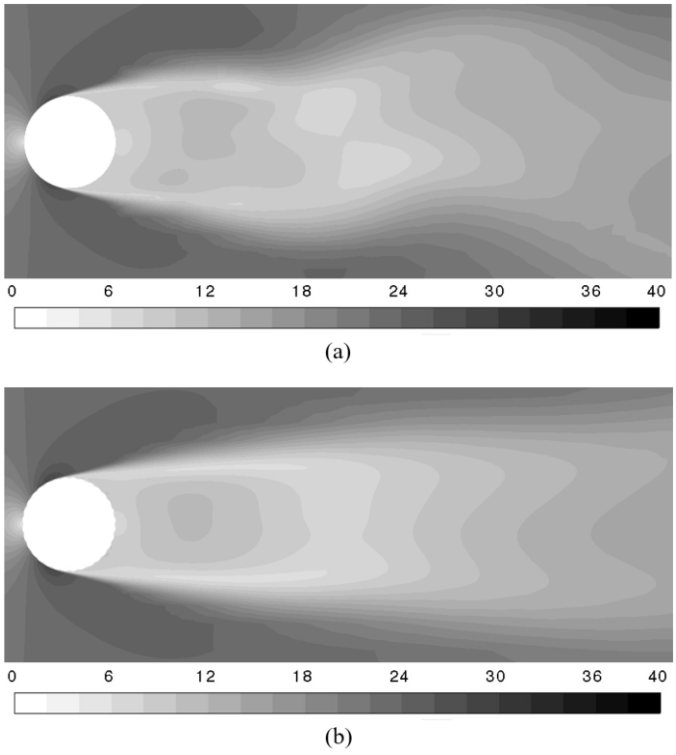

Fig. 21 Velocity magnitude (m/s) cut plot of wake region through center of 3D circular cylinder for the (a) smooth case and
(b) Model A

Conclusion

In circular and elliptical cylinders, surface grooves perpendicular to the flow reduce the drag experienced by the cylinder due by producing turbulent or laminar vortices in grooves and decreasing the angle of separation of boundary layer which makes the wake region smaller and reduces the drag. Such drag reduction is observed in two- and three-dimensional flow.

Acknowledgements

The authors thank Cedarville Professor of Mechanical Engineering, Dr. Zhaohui (George) Qin for his leadership and advising of the students throughout the research process. They also thank Cedarville Dean of the School of Engineering and Computer Science, Dr. Robert Chasnov, for supplying the resources necessary to fabricate and test the physical models. They also thank Cedarville Professor Emeritus, Dr. Hardwood Hegna for training and assistance in obtaining accurate, consistent experimental data from the wind tunnel.

Bibliography

[1] X. Song, Y. Qi, M. Zhang, G. Zhang, and W. Zhang, "Application and optimization of arag reduction characteristics on the flow around a partial grooved cylinder by using the response surface method," *Engineering Applications of Computational Fluid Mechanics,* vol. 13, no. 1, pp. 158-176, Jan. 2019.

[2] I. Rodriguez, et al, "LES-based study on the roughness effects on the wake of a circular cylinder from subcritical to transcritical Reynolds numbers," *Flow Turbulence and Combustion,* vol. 99, no. 3-4, pp. 729-763, Oct. 2017.

[3] G. Buresti, "The effect of surface roughness on the flow regime around circular cylinders," *Journal of Wind Engineering and Industrial Aerodynamics*, vol. 8, no. 1-2, pp. 105-114, 1981.

[4] S. H. Seo, C. D. Nam, J. Y. Han, and C. H. Hong, "Drag reduction of a bluff body by grooves laid out by design of experiment," *Journal of Fluids Engineering-Transactions of the ASME*, vol. 135, no. 11, Nov. 2013.

[5] G. Yunqing, L. Tao, M. Jeigang, S. Zhengzan, and Z, Peijian, "Analysis of drag reduction methods and mechanisms of turbulent," *Applied Bionics and Biomechanics,* vol. 2017, article ID 6858720, pp. 1-8, 2017.

[6] M. Bird, et al, "SAE Aero Design 2016-2017," (unpublished), Cedarville, OH, 2017.

[7] B. R. Munson, *Fundamentals of Fluid Mechanics.* 7th ed. Hoboken, NJ: John Wiley & Sons, Inc, 2013.

[8] Ohio Supercomputer Center. 1987. Ohio Supercomputer Center. Columbus OH: Ohio Supercomputer Center.

[9] W. Wang, J. Wang, H. Liu, and B. Y. Jiang, "CFD prediction of airfoil drag in viscous flow using the entropy generation method," *Mathematical Problems in Engineering,* vol. 2018, article ID 4347650, May 2018.

[10] X. Song, P. Lin, R. Liu, and P. Zhou, "Skin Friction Reduction Characteristics of Variable Ovoid Non-Smooth Surfaces," *Journal of Zhejiang University-Science A,* vol. 18, no. 1, pp. 59-66, 2017.